

Tuning Shape Parameter of Radial Basis Functions in Zooming Images using Genetic Algorithm

A. M. Esmaili Zaini¹, A. Mohammad Latif^{2,*} and Gh. Barid Loghmani¹

Department of Applied Mathematics, Yazd University, Yazd, Iran.

Department of Computer Engineering, Yazd University, Yazd, Iran.

Received 21 September 2016; Revised 20 December 2016; Accepted 09 July 2017

*Corresponding author: alatif@yazd.ac.ir (A. Latif).

Abstract

Image zooming is one of the current issues of image processing that maintains the quality and structure of an image. In order to zoom an image, it is necessary to place the extra pixels in the image data. Adding the data to the image must be consistent with the texture in the image in order to prevent artificial blocks. In this work, the required pixels are estimated using the radial basis functions and calculating the shape parameter c with the genetic algorithm. Then all the estimated pixels are revised on the basis of the sub-algorithm of edge correction. The proposed method is a non-linear one that preserves the edges and minimizes the blur and block artifacts on the zoomed image. This method is evaluated on several images for calculating the suitable shape parameter of the radial basis functions. The numerical results obtained are presented using the PSNR and SSIM fidelity measures on different images as compared to some other methods. The average PSNR of the original image and image zooming was found to be 33.16, which shows that image zooming by factor of 2 is similar to the original image, which emphasizes that the proposed method has an efficient performance.

Keywords: *Image Zooming, Radial Basis Function, Genetic Algorithm, Interpolation.*

1. Introduction

Image zooming is used to enhance the resolution of an image in order to achieve a high-quality image. It plays an important role in image processing and machine vision, and has a variety of applications in the printing industry, electronic publishing, digital cameras, medical imaging and sampling, images on web pages, license plate recognition, and face recognition systems [1].

Recent studies have shown that in many applications the main task regards the visual quality of images. Resolution of the edges and lack of blurred and additional artifacts are two important factors involved in the quality of zoomed images.

In most algorithms of image zooming, the interpolation method is used. This is to find a set of unknown pixel values from a set of known pixel values in the image.

In image zooming, several basic parameters affect the image quality, as follow [2]:

1. The zooming method should maintain the edges and borders of the image.

2. The method should not produce constant undesirable pieces or blocks of other areas.
3. The method should involve efficient computations, and it should not depend on the inner parameters too much.

Traditional technologies use linear interpolation methods to create high resolution samples in zooming images. Pixel replication, bi-linear interpolation, quadratic interpolation, bi-cubic interpolation, and spline interpolation are among the linear interpolation methods [3-5]. These methods serve to smooth out image edges, and, in some cases, to produce stair edges. Also the outputs of these methods are blurred images.

In the bi-linear interpolation method, artificial blocks and undesirable visual effects appear at a high zooming rate, and the edges are preserved to an acceptable degree.

In the bi-cubic interpolation method, at a suitable zooming rate, the artificial blocks and the undesirable visual effects are fewer than in the bi-

linear interpolation method, and the edges are preserved as well. Determining the image quality in these methods is difficult but in terms of high quality, one may refer to the spline interpolation, bi-cubic interpolation, quadratic interpolation, and bi-linear interpolation methods in a descending order [6].

To modify the linear methods in terms of improving the image quality and solving the problem of image blur, the non-linear interpolation technique has been used. The changes in the non-linear methods depend on their interpolation. This means that the performance of these methods with sharp edges is different from their performance with soft edges. Indeed, it is in contrast with the linear methods that treat all pixels equally [7-9].

In non-linear methods, a subset of edge pixels is estimated [8], and resampling, parameter optimization, contextual interpolation, and edge direct interpolation are conducted to preserve the image quality and edges [10-13].

In reference [10], statistical methods have been used to set the structure of the edges and the correction technique of bi-linear interpolation, and the interpolation error theorem [11] have been used in the edge-adaptive method.

In reference [14], as a part of the edge-directed non-linear interpolation method, the technique of filtering direction and data fusion has been used, and a missed pixel has been interpolated in different directions. Then the results of edge-directed interpolation have been combined with the linear least squares estimation, and thus the desirable outcome has been achieved.

In reference [15], the LAZ method has been introduced as a local adaptive zooming algorithm in order to find the edges in different directions using the information of discontinuity or sharp brightness changes. Also two threshold values have been considered, and the missed pixels have been estimated regarding the direction of the edge.

In the recent years, some methods based on the partial differential equations (PDEs) have been proposed and have shown better performance than the previous methods. In references [16 and 17], the edge-directed interpolation methods have been discussed based on the diverse issues with PDEs.

In reference [18], the non-linear curvature interpolation method and PDEs for image-zooming have been provided.

In reference [19], the non-linear fourth-order PDEs method is a combination of the locally adaptive zooming algorithm for image zooming.

In reference [20], an image zooming algorithm has been presented using non-linear PDE combined with edge-directed bi-cubic algorithm.

Most PDE-based methods provide clear images with sharp edges. The effects resulting from blurring and the artificial blocks are minimized in these methods.

In reference [21], a non-linear image-zooming method has been provided based on the radial basis functions and the contextual edge correction techniques. Given that the radial basis functions have the shape parameter c in this method, an interval has been proposed for c by performing numerical experiments.

In reference [22], the artificial neural network methods have been used for zooming operations on digital images.

In reference [23], a non-linear image interpolation algorithm based on the moving least squares technique has been presented. In this method, ability for image zooming and preserving edge features is demonstrated.

In reference [24], image magnification by least squares surfaces has been presented in such a way that extra pixels are estimated using the surface of least squares.

In the present work, using the Genetic Algorithm (GA) and the measure of similarity of two images, the required pixels were calculated regarding the radial basis functions, and the shape parameter c was desirably obtained. Then all the estimated pixels were revised based on the proposed edge correction sub-algorithm.

The structure of this paper is as what follows. In Section 2, the radial basis functions and their properties are discussed. In Section 3, GA and image zooming are briefly reviewed. In Section 4, the proposed method is provided. In Section 5, the evaluation criteria and the results of running and calculating the shape parameter c are discussed using GA in radial basis functions and compared with other methods. In the final part, the conclusion and the future research works in this field are given.

2. Radial basis functions

Radial basis functions play a key role in various fields of engineering and applied mathematics including functions in the discussion of interpolation and solving partial differential equations. Solving a high-dimensional interpolation problem is not as easy as solving univariate functions because the amount of calculations and the complexity of the algorithm are high. According to Hardy [25], a multivariate interpolating function is not unique.

Due to these obstacles, Hardy [26] provided new-basis functions in 1971. Later, on the basis of this provision, radial basis functions emerged as a standard method of approximation. These functions and their importance and applied properties are defined as follow:

Definition 1-2: function $\phi: R^n \rightarrow R$ is called ‘radial function’ if $\|x\| = \|y\|$, then $\phi(x) = \phi(y)$, where $\|\cdot\|$ is the Euclidean norms. in fact, suppose that $\bar{X} = (x_1, x_2, \dots, x_d) \in \Omega \subseteq R^d$ and $\phi: R^d \rightarrow R$. Then $\bar{X} = (x_1, \dots, x_d) \rightarrow \phi(\|x_1, \dots, x_d\|_2)$, where

$$\|\bar{X}\|_2 = \sqrt{\sum_{i=1}^d X_i}$$

$\|\bar{X}\|_2$ is the distance of \bar{X} from the origin. Thus the above functions are called ‘radial functions’ because the discussion is on the distances of the points from a particular center that is the origin.

If the constant points $\bar{x}_1, \bar{x}_2, \dots, \bar{x}_n \in R^d$ are given and the following linear composition is displayed from the functions g to the center of the points \bar{x}_i :

$$f: R^d \rightarrow R$$

$$\bar{x} \rightarrow \sum_{i=1}^n \alpha_i g(\bar{x} - \bar{x}_i) = \sum_{i=1}^n \alpha_i \phi(\|\bar{x} - \bar{x}_i\|) \tag{1}$$

where, $\|\bar{x} - \bar{x}_i\|$ is an Euclidean norm between the points \bar{x}, \bar{x}_i , ϕ , is the radial basis function, and α_i is the real coefficient. Then function f can be displayed as (2). Also the obtained function f is placed in a space composed of the radial basis functions with a finite dimension.

$$f(\bar{x}) = \sum_{i=1}^n \alpha_i \phi(\|\bar{x} - \bar{x}_i\|) \tag{2}$$

Definition 2-2: we suppose a set of n distinct points $\{x_i\}_{i=1}^n$ with the corresponding distinct values $\{f_i\}_{i=1}^n$ given. In this case, the interpolating function is defined as (3) using the radial basis function.

$$s(x) = \sum_{i=1}^n \lambda_i \phi(\|x - x_i\|) \tag{3}$$

where, the interpolation condition is:

$$S(x_i) = f(x_i), \quad i = 1, 2, \dots, n.$$

Equation (3) is equivalent with the linear equations system (4), where the coefficient λ_i can be calculated.

$$A\lambda = F \tag{4}$$

where

$$A = \begin{pmatrix} \phi(\|x_1 - x_1\|) & \phi(\|x_1 - x_2\|) & \dots & \phi(\|x_1 - x_n\|) \\ \phi(\|x_2 - x_1\|) & \phi(\|x_2 - x_2\|) & \dots & \phi(\|x_2 - x_n\|) \\ \vdots & \vdots & \ddots & \vdots \\ \phi(\|x_n - x_1\|) & \phi(\|x_n - x_2\|) & \dots & \phi(\|x_n - x_n\|) \end{pmatrix}$$

A is an interpolating matrix of $n \times n$ with the element $A_{ij} = \phi(\|x_i - x_j\|)$, $i, j = 1, \dots, n$.

In addition,

$$\lambda = \begin{pmatrix} \lambda_1 \\ \lambda_2 \\ \vdots \\ \lambda_n \end{pmatrix}, \quad F = \begin{pmatrix} f_1 \\ f_2 \\ \vdots \\ f_n \end{pmatrix}$$

In matrix A , ϕ s are radial basis functions, and it is clear that matrix A is a symmetric matrix regarding the radial basis function.

Shoenberg [27] has proved that any non-constant function $\phi: [0, \infty) \rightarrow R$ is strictly positive definite if and only if the function $\psi: r \rightarrow \phi(\sqrt{r})$ on $[0, \infty)$ is completely monotonic. In his article, Michely [28] has shown that if $\phi \in C^\infty[0, \infty)$ and ϕ' are completely monotonic and non-constant, and $\phi(0) \geq 0$, then matrix A is non-singular for each $\psi(r) = \phi(\sqrt{r})$.

If the positive definite radial basis functions are used to form matrix A , then A is positive definite and the system always has a solution. However, if the conditional positive definite radial basis functions are used to form matrix A , the interpolating system will be in a specific form; according to (3), if ϕ s are the positive definite

functions with the order Q where $q = \binom{Q-1+d}{d}$,

then with the condition in which:

$$s(x) = \sum_{i=1}^n \lambda_i \phi(\|x - x_i\|) + \sum_{k=1}^q B_k P_k(x) \tag{5}$$

$$\sum_{i=1}^n \lambda_i P_k(x_i) = 0, \quad 1 \leq k \leq q \tag{6}$$

Equations (5) and (6) are converted to matrix (7):

$$\begin{pmatrix} A & P \\ P^T & 0 \end{pmatrix} \begin{pmatrix} \lambda \\ B \end{pmatrix} = \begin{pmatrix} F \\ 0 \end{pmatrix} \tag{7}$$

where, $A_{ij} = \phi(\|x_i - x_j\|)$ for $i, j = 1, \dots, n$ and $P_{ij} = P_j(x_i)$ are the assumptions of the interpolating matrix A , for a given ϕ .

Using this trick, the new matrix is non-singular, and the system will have a solution without any damage to the generality of the problem of interpolation.

In general, the radial basis functions are classified into two groups: extremely smooth functions and piecewise smooth functions. Table 1 shows some extremely smooth and piecewise functions.

In extremely smooth radial basis functions, $c > 0$ is a shape parameter that plays a key role in the accuracy of the methods based upon these functions. Finding the optimal parameters has been considered for many years and they are often calculated through trial and error. Selecting an appropriate c often depends on the problem, and c cannot be selected with certainty.

3. Genetic algorithm and image zooming

Genetic algorithm (GA) is used as a method for finding suitable solutions to most engineering and

optimization problems. This algorithm, which uses the evolutionary computation to find suitable solutions, has been inspired by the Darwinian evolutionary theory. This algorithm has been developed by Holland [29], starting with a completely random population and going on through generations. In each generation, the entire population is evaluated, based on the principal of the survival of the fittest, and the better results are selected based on the targeted function (fitness) and transmitted to a new generation. This process is repeated until the termination condition of the algorithm is established. Choosing a fitness function in GA is very important. Therefore, it must be proportionate to the problem. This algorithm leads to suitable solutions by using the operators of selection, cross-over, and mutation.

Table 1. Radial basis function.

Name of function	Type of function	$\phi(r)$
Gaussian function	Extremely smooth	e^{-cr^2}
Multiple quadratic	Extremely smooth	$\sqrt{c^2 + r^2}$
Reverse quadratic	Extremely smooth	$\frac{1}{c^2 + r^2}$
Reverse multiple quadratic	Extremely smooth	$\frac{1}{\sqrt{c^2 + r^2}}$
Linear spline	Piecewise smooth	r
Cubic spline	Piecewise smooth	r^3
Thin plate spline	Piecewise smooth	$r^2 \ln r$

In image zooming, a number of new pixels are placed among the original pixels of the image. In zooming, the aim is to estimate the amount of new pixels, which is determined on the basis of their neighboring pixels. There are two kinds of neighborhoods in 2D images, namely 4-cell and 8-cell neighborhoods. These neighborhoods are shown in figure 1. In most of the proposed methods, attempt is made to keep the zooming rate at a power of two but it should be noted that this algorithm is usable for every zooming rate.

Suppose that the dimensions of the original image, $n \times n$, spread regularly to $2n \times 2n$.

More precisely, if $S(i, j)$ represents the pixel of the original image in the i^{th} row, and the j^{th} column

and $Z(l, k)$ represent the pixel of the zoomed image in the l^{th} row and the k^{th} column, then function f defined by (8) places the values for the original image pixels in the interlaced places of the new image.

$$f : S \rightarrow Z$$

$$f(S(i, j)) = Z(2i - 1, 2j - 1) \tag{8}$$

$$i, j = 1, 2, \dots, n$$

The result is shown in figure 2. The original image pixels are shown with \bullet , and the other pixels that must be estimated in three steps are shown with \circ . These steps estimate the pixels with even columns and even rows, odd rows and even columns, and even rows and odd columns. In

order to estimate the values for these pixels, the radial basis functions and the related linear system are used, and then all the pixels are revised with the edge-modified sub-algorithm.

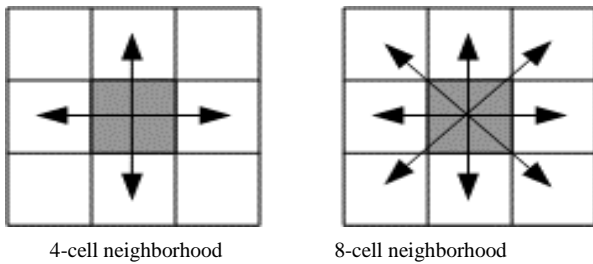


Figure 1. Types of neighborhoods.

For the image zooming by factor of 4, the original image expands to the image according to figure 2. Then all the required pixels are estimated. This process is repeated once more.

4. Proposed method

In this method, the points are referred to the pixel coordinate of the image whose brightness and



Figure 2. Image zooming.

Step 5. The intended pixels are estimated by replacing the number of columns and rows in the radial basis function.

Step 6. Steps 3 to 5 in three stages are repeated according to the zooming algorithm and estimating the required pixel.

Step 7. The measure PSNR or SSIM of the original image with the zoomed image is calculated.

Step 8. If the stop condition is satisfied, go to step 9; otherwise, go to step 2.

Step 9. The suitable parameter *c* of the radial basis function in zooming the images with regard to the termination condition in GA is determined.

Step 10. All the estimated pixels, again based on the directed edge sub-algorithm, are revised (explained in the next part).

4.1. Modified sub-algorithm of image edges

After estimating all the required pixels, they are revised to improve the edges, as shown in figure

number of columns and rows are considered as a point in a 3D space. In order to estimate the required pixels based on the 4-cell neighborhood, the intended point is selected, and then the intended pixels are estimated by selecting the radial basis function and solving the related linear system by (4).

Thus the shape parameter *c* is determined in the radial basis function with GA.

The flow chart of the proposed method is shown in figure 3. It should be noted that to approximate the pixels of the last column and row, the penultimate row and column are repeated.

The steps of the proposed algorithm are as follow: Step 1. The radial basis function is selected.

Step 2. GA is called to determine the random shape parameter *c*.

Step 3. The linear equation system with regard to the selected radial basis function is formed.

Step 4. The linear equation system and the coefficient are solved.

4. Based upon the following conditions, they are modified if required [15]. *A*, *B*, *C*, and *D* are the original pixels, and *X*, *Y*₁, *Y*₂, *Z*₁, and *Z*₂ are the estimated pixels. The advantage of this sub-algorithm is that there is no threshold for the image edges. The steps of the proposed sub-algorithm are as follow:

Step 1. If $|A - D| > |B - C|$, then $X \leftarrow \frac{B + C}{2}$. In fact, the edge is in the NE-SW direction.

Step 2. If $|A - D| < |B - C|$, then $X \leftarrow \frac{A + D}{2}$. In fact, the edge is in the NW-SE direction.

Step 3. If $(A - D)(B - C) > 0$ then $Y_1 \leftarrow \frac{A + B}{2}$ and $Y_2 \leftarrow \frac{C + D}{2}$. In fact, the edge is in the NS direction.

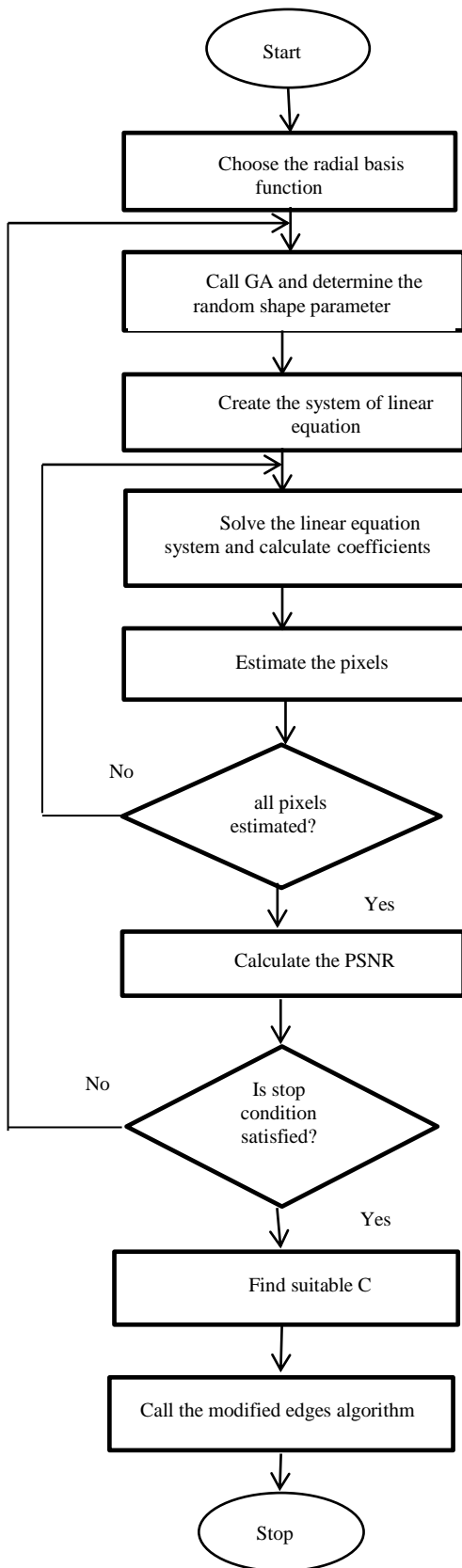


Figure 3. A flow chart of proposed algorithm.

Step 4. If $(A - D)(B - C) < 0$ then $Z1 \leftarrow \frac{A + C}{2}$ and $Z2 \leftarrow \frac{B + D}{2}$. In fact, the edge is in the EW direction.

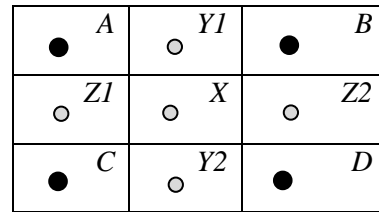


Figure 4. A design for correcting edges.

5. Experimental results

In order to evaluate the proposed method, for image zooming by factor of 2, a digital image was first considered as an original image, and then reduced to half its size by removing its rows and columns alternately. Next, it was enlarged to double its size using the proposed method and the other existing methods. As it was expected, the more similar the original and the zoomed images, the better the performance of the algorithm. In the next section, evaluation of quality metrics is presented.

5.1. Assessment criteria

The PSNR and SSIM criteria are used to compare two images in terms of their similarity. The greater the amount of PSNR and the closer the amount of SSIM is to one, the more is the conformity of the two images [30]. The measure PSNR is calculated on the basis of (9) and (10):

$$PSNR = 10 * \log_{10} \left(\frac{MAXI^2}{MSE} \right) \quad (dB) \quad (9)$$

$$MSE = \frac{1}{m \cdot n} \sum_{i=0}^{m-1} \sum_{j=0}^{n-1} [I(i,j) - K(i,j)]^2 \quad (10)$$

where, $I(i, j)$ and $K(i, j)$ are the pixels of the original image and the estimated image, respectively, and $MAXI$ is the maximum amount of the image pixels.

The measure SSIM, which includes the structural elements of the picture, measures the quality of the structural content and the similarity between the two images, that is a number between zero and one, and is calculated by (11). The closer the measure is to one, the more similar the two images are. However, the closer the measure is to zero, the less similar the two images are.

$$SSIM(x,y)=\frac{(2\mu_x\mu_y+c_1)(2\sigma_x\sigma_y+c_2)(\sigma_{xy}+c_3)}{(\mu_x^2+\mu_y^2+c_1)(\sigma_x^2+\sigma_y^2+c_2)(\sigma_x\sigma_y+c_3)} \quad (11)$$

where, μ , σ^2 and σ_{xy} are the mean, variance, and co-variance of the pixels, respectively, and c_1 , c_2 , and c_3 are three constants to prevent the denominator from being zero.

5.2. Numerical experiments of proposed method

The shape parameter c of radial basis function is determined using GA. Important parameters in GA are shown in table 2.

Table 2. GA setting.

Scaling function	Rank
Cross-over rate	0.8
Mutation rate	0.2
Mutation function	Adaptive feasible
Cross-over function	Constraint dependent
Selection function	Uniform

The results of running the proposed algorithm in the MATLAB software were tabulated in tables 3 and 4. In table 3, the measures PSNR and SSIM were used to zoom the image. Also 10 different standard images are shown in figure 5, in which their size is 512×512 [31].



Figure 5. Different standard images for image zooming.

The results of the proposed method were obtained using the extremely smoothly Gaussian radial basis function e^{-Cr^2} (GRBF). In GA, the used range was $[-10, 10]$, and the initial population was considered to be 10. However, a better number of population was considered to be 5 so that the next

generation would be continued regarding the values for PSNR and SSIM.

For the proposed images, on average, the termination condition was achieved after 70 repetitions. After running the algorithm, a suitable value for c was found to be 2.4335. Figure 6 shows the process of reaching a suitable solution in zooming the image with GA.

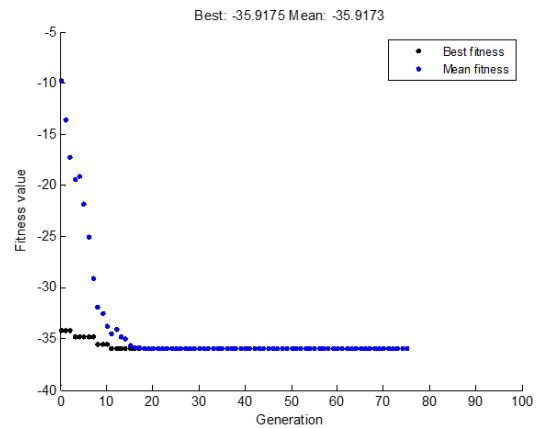


Figure 6. Process of reaching a suitable solution using GA and GRBF in image of lifting body.

It should be noted that PSNR was used in the algorithm because in a GA, the minimum value for the targeted function is calculated. After running the algorithm and calculating a suitable value for the shape parameter c , the sub-algorithm of edge correction was run on the image.

The results obtained were tabulated in table 3. The minimum difference of PSNR by the GRBF method with edge correction and without edge correction was 0.08 and the maximum was 0.47, whilst the average was 0.21. Also it could be seen that the quality of the images was preserved at a desirable level.

Table 4 shows the results of implementing the proposed method using the extremely smoothly reverse quadratic radial basis function $\frac{1}{c^2+r^2}$ (RQRBF). In GA, the applied range was $[0,100]$, and the initial population was considered to be 20; however, a better number of population was considered to be 10 so as to the next generation to continue with regard to the values for PSNR and SSIM.

For the proposed images, on average, the termination condition was achieved after 51 repetitions. A suitable value for c , obtained after running the algorithm, is shown in table 3. Figure 7 shows the process of reaching a suitable solution in zooming the image with GA. After running the algorithm and calculating the optimal value for the shape parameter c , the directed edge sub-algorithm was run on the image.

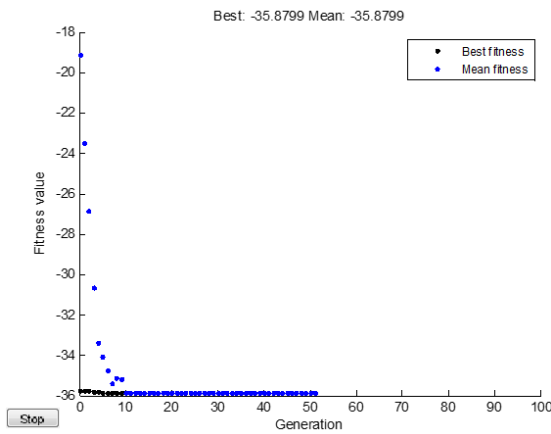


Figure 7. Process of reaching a suitable solution using GA and QRBF in image of lifting body

The results obtained were tabulated in table 4. The least difference of PSNR between with and without edge correction by the QRBF method was 0.07, the most was 0.51, and its average was 0.21. As it can be seen, the quality of the images is preserved at a desirable level.

According to the results obtained, it can be concluded that a suitable value for the shape parameter c in the Gaussian radial basis function is independent from the image but the reverse quadratic radial basis function depends on it.

Table 3. Results of running GRBF with suitable c on different images using SSIM and PSNR, with and without edge correction by factor of 2 in zooming.

Methods images	Without edge correction		With edge correction	
	SSIM	PSNR	SSIM	PSNR
Lifting body	0.9766	35.92	0.9769	36.39
Elaine	0.9601	34.58	0.9589	34.66
Disk	0.9952	33.00	0.9956	33.08
Fire	0.9850	32.09	0.9857	32.21
Swan	0.9835	33.09	0.9842	33.22
Dog	0.9806	33.78	0.9814	33.94
Balloons	0.9889	32.31	0.9894	32.55
House	0.9860	33.83	0.9867	33.99
Airplane	0.9792	29.65	0.9812	29.95
Fruits	0.9616	31.24	0.9608	31.59

Table 4. Results of running QRBF with suitable c on different images using SSIM and PSNR, with and without edge correction by factor of 2 in zooming.

Methods images	Without edge correction		With edge correction		suitable values of the shape parameter c
	SSIM	PSNR	SSIM	PSNR	
Lifting body	0.9766	35.88	0.9769	36.39	12.781
Elaine	0.9601	34.59	0.9589	34.66	17.875
Disk	0.9952	33.00	0.9956	33.08	0.607
Fire	0.9850	32.10	0.9857	32.21	18.625
Swan	0.9835	33.08	0.9842	33.22	20.026
Dog	0.9806	33.78	0.9814	33.94	17.688
Balloons	0.9890	32.34	0.9893	32.57	10.188
House	0.9860	33.86	0.9867	34.00	13.75
Airplane	0.9792	29.67	0.9812	29.97	12.938
Fruits	0.9617	31.24	0.9608	31.59	14.871

5.3. Comparison of results of proposed method with other methods

In order to evaluate the proposed algorithm, the results were obtained using the extremely smoothly GRBF e^{-Cr^2} . This was compared with non-linear PDE with edge directed bi-cubic (PDEWBC) [20] and least square ellipsoid (LSE) methods [24], bi-linear interpolation (BIL) method, bi-cubic interpolation (BIC) method, and curvature interpolation method (CIM) [18].

The results obtained are presented in table 5. As one can see in this table, the average difference of PSNR between the GRBF and LSE methods is

0.24, between GRBF method and PDEWBC is 1.33, and between the GRBF method and CIM is 1.75. Also the average difference of PSNR between the GRBF and BIC methods is 2.26, and between the GRBF and BIL method is 2.16.

With regard to comparison of the results, it can be concluded that the proposed GRBF method has a better performance than the other methods on the selected image.

It is to emphasize that the results are also obtained by zooming factor of 4 with GRBF with suitable c , as shown in table 6.

Table 5. Comparison of GRBF and other methods by PSNR criterion by factor of 2 in zooming.

Methods						
images	BIL	BIC	CIM	PDEWBC	LSE	GRBF
Lifting body	33.34	33.30	33.87	34.41	36.17	36.39
Elaine	31.26	31.08	31.49	31.80	34.61	34.66
Disk	30.94	30.82	31.56	31.93	32.70	33.08
Fire	31.66	31.71	31.82	31.97	31.95	32.21
Swan	31.19	30.74	31.44	31.88	32.73	33.22
Dog	31.83	31.37	32.05	32.65	33.63	33.94
Balloons	31.29	31.73	32.28	32.77	34.07	32.55
House	32.64	32.60	32.97	33.24	33.83	33.99
Airplane	29.70	29.59	30.12	30.49	31.30	29.95
Fruits	26.17	26.08	26.49	27.12	28.20	31.59
Average	31.00	30.90	31.41	31.83	32.92	33.16

Table 6. Results of running GRBF using PSNR, with edge correction and compare other methods by factor of 4 in zooming.

Methods					
images	BIL	BIC	CIM	PDEWBC	GRBF
Lifting body	27.39	27.05	27.89	28.41	30.43
Elaine	26.49	26.14	28.49	29.21	30.68
Disk	25.77	25.56	26.68	28.74	30.92
Fire	25.60	25.46	25.71	26.02	26.08
Swan	26.90	26.75	26.93	26.98	26.37
Dog	27.55	27.38	27.61	27.85	27.68
Balloons	24.94	24.75	25.34	25.76	26.28
House	27.09	26.90	27.56	28.06	28.84
Airplane	22.49	22.12	23.85	24.34	25.16
Fruits	23.07	22.72	24.23	25.16	26.99
Average	25.73	25.48	26.43	27.06	27.94

These results were compared with the BIL, BIC, CIM, and PDEWCB methods. As indicated in table 6, the PSNR value, average difference of PSNR between the GRBF and BIL methods is 2.21, between the GRBF and BIC methods is 2.46, between the GRBF method and CIM is 1.51, and between the GRBF and PDEWBC methods is 0.88. The merit of the presented method is that

the objective evaluation results are better than the performance of the other methods.

From a visual perspective, figure 8 shows the sample image Elaine zoomed with the proposed method and in two modes with and without edge correction. The images obtained from the proposed method are clearer and blur less with good performance on the edges.

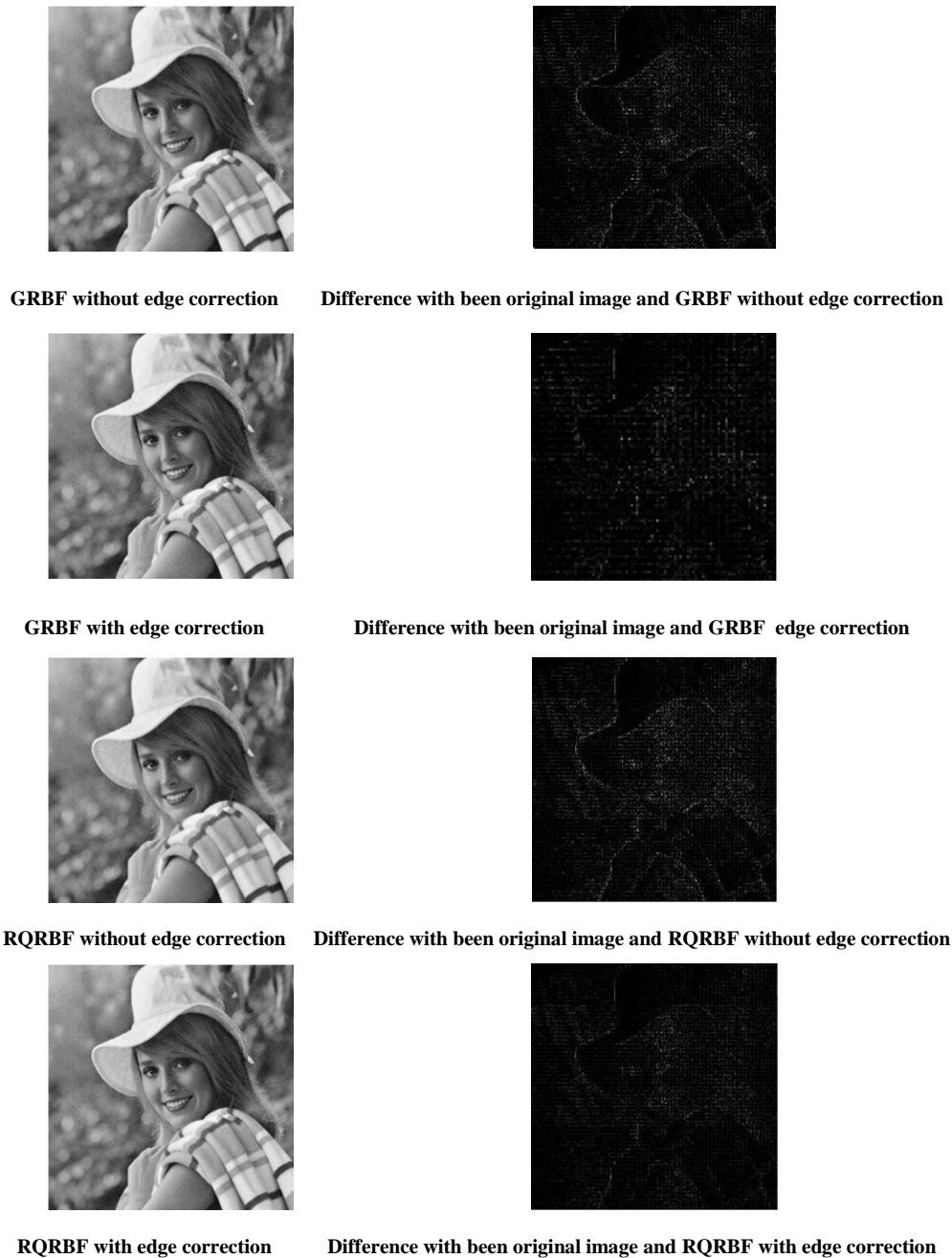


Figure 8. Results of Elaine's image zooming by factor of 2 and using different methods.

6. Conclusion

In this research work, a suitable value for the shape parameter c was achieved by radial basis functions with the application of GA. This

achieved result has been used in zooming images. This method provided desirable results.

In addition, the edge correction technique was used to enhance the quality of images after calculating a suitable value for the shape

parameter c . In the future studies, the proposed method can be developed with other edge correction techniques or non-linear methods such as the two-variable interpolation method or a combination of radial basis function isolation and edge correction techniques. It is to note that proving the independence of the shape parameter c in the Gaussian radial basis function in zooming images will be investigated in our future research project.

References

- [1] Lehmann, T., Gönner, C. & Spitzer, K. (1999). Survey: Interpolation methods in medical image processing, *IEEE Trans. Med. Imaging.*, vol. 18, no. 11, pp. 1049–1075.
- [2] Lee, Y. J. & Yoon, J. (2010). Nonlinear image upsampling method based on radial basis function interpolation, *IEEE Trans. Image Process.*, vol. 19, no. 10, pp. 2682–2692.
- [3] Keys, R. G. (1981). Cubic convolution interpolation for digital image processing, *IEEE Trans. Acoust., Speech, Signal Process.*, vol. 29, no. 6, pp. 1153–1160.
- [4] Hou, H. S. & Andrews, H. C. (1978). Cubic splines for image interpolation and digital filtering, *IEEE Trans. Acoust., Speech, Signal Process.*, vol. 26, no. 6, pp. 508–517.
- [5] Thévenaz, P., Blu, T. & Unser, M. (2000). Interpolation revisited, *IEEE Trans. Med. Image.*, vol. 19, no. 7, pp. 739–758.
- [6] Padmanabhan, S. A. & Chandramathi, S. (2011). Image zooming using segmented polynomial interpolation in R^2 space, *European Journal of Scientific Research*, vol. 57, no. 3, pp. 447-453.
- [7] Jensen, K. & Anastassion, D. (1995). Subpixel edge localization and the interpolation of still images, *IEEE Trans. Image Process.*, vol. 4, no. 3, pp. 285–295.
- [8] Allebach, J. & Wong, P. W. (1996). Edge-directed interpolation, in *Proc. IEEE Int. Conf. Image. Proc.*, vol. 3, pp. 707–710.
- [9] Carrato, S. & Tenze, L. (2000). A high quality 2X image interpolator, *IEEE Signal Process.*, vol. 7, no. 6, pp. 132–135.
- [10] Li, X. & Orchard, T. (2001). New edge directed interpolation, *IEEE Trans. Image Process.*, vol. 10, no. 10, pp. 1521–1527.
- [11] Cha, Y. & Kim, S. (2007). The error-amended sharp edge (ease) scheme for image zooming, *IEEE Trans. Image Process.*, vol. 16, no. 6, pp. 1496–1505.
- [12] Li, M. & Nguyen, T. Q. (2008). Markov random field model-based edge directed image interpolation, *IEEE Trans. Image Process.*, vol. 17, no. 7, pp. 1121–1128.
- [13] Zhang, X. & Wu, X. (2008). Image interpolation by adaptive 2-D autoregressive modeling and soft-decision estimation, *IEEE Trans. Image Process.*, vol. 17, no. 6, pp. 887–896.
- [14] Zhang, L. & Wu, X. (2006). An edge-guided image interpolation algorithm via directional filtering and data fusion, *IEEE Trans. Image Process.*, vol. 15, no. 8, pp. 2226–2238.
- [15] Battiato, S., Gallo, G. & stanco, F. (2002). A locally adaptive zooming algorithm for digital images, *Image and Vision Computing*, vol. 20, no. 11, pp. 805-812.
- [16] Jiang, H. & Moloney, C. (2002). A new direction adaptive scheme for image interpolation, in *Proc. Int. Conf. Image Processing*, vol. 3, pp. 369-372.
- [17] Wang, Q. & Ward, R. K. (2007). A new orientation-adaptive interpolation method, *IEEE Trans. Image Process.*, vol. 16, no. 4, pp. 889–990.
- [18] Kim, H., Cha, Y. & Kim, S. (2011). Curvature interpolation method for image zooming, *IEEE Trans. Image Process.*, vol. 20, no. 7, pp.1895-1903.
- [19] Nowrozian, N. & Hassanpour, H. (2014). Image zooming using non-linear partial differential equation, *International Journal of Engineering Transactions A: Basics*, vol. 27, no. 1, pp. 15-28.
- [20] Warbhe, S. & Gomes, J. (2016). Interpolation technique using non-linear partial differential equation with edge directed bi-cubic, *International Journal of Image Processing*, vol. 10, no. 4, pp. 205-213.
- [21] Lee, Y. J. & Yoon, J. (2010). Nonlinear image upsampling method based on radial basis function, *IEEE Trans. Image Process.*, vol. 19, no. 10, pp. 2682–2692.
- [22] Youssef, D., Mohammed, B., Abdelmalek, A., Tarik, H. & EL Miloud, J. (2015). Zoom and restoring of digital image artificial neural networks, *Computer Science and Engineering*, vol. 5, no. 1, pp. 14-24.
- [23] Lee, Y.J. & Yoon, J. (2015). Image zooming method using edge-directed moving least squares interpolation based on exponential polynomials, *Applied Mathematics and Computation*, vol. 269, pp. 569-583.
- [24] Esmaili Zaini, A. M., Barid Loghmani, G. & Latif, A. M. (2016). Image magnification by least squares surfaces, *Iranian Journal of Numerical Analysis and Optimization*. In press.
- [25] Watson, G. A. (1980). *Approximation theory and numerical methods*, Wiley.
- [26] Hardy, R. L. (1971). Multiquadric equations of topology and other irregular surface, *J. Geophys. Res.*, vol. 76, pp. 1905-1915.
- [27] Schoenberg, I. J. (1970). Matric space and completely monotone functions, *Ann. Math. Appl.* vol. 23, pp. 811-841.

[28] Michelli, C. A. (1986). Interpolation of scattered data distance matrices and conditionally positive definite functions, *Constr. Approx.*, vol. 2, pp.11-22.

[29] Holland, J. H. (1992). *Adaptation in natural and artificial systems*. 1975. Ann Arbor, MI: University of Michigan Press and.

[30] Wang, Z., Bovik, A. C., Sheikh, H. R. & Simoncelli, E. P. (2004). Image quality assessment: from error visibility to structural similarity, *IEEE Trans. Image Process.*, vol. 13, no. 4, pp. 600-612.

[31] Online. Available: www.freeimages.co.uk and sipi.usc.edu/database.

تنظیم پارامتر شکل توابع پایه شعاعی در بزرگ‌نمایی تصویر با استفاده از الگوریتم ژنتیک

علی محمد اسمعیلی زینی^۱، علی محمد لطیف^{۲*} و قاسم برید لقمانی^۱

^۱ دانشکده ریاضی، دانشگاه یزد، یزد، ایران.

^۲ گروه مهندسی کامپیوتر، دانشگاه یزد، یزد، ایران.

ارسال ۲۰۱۶/۹/۲۱؛ بازنگری ۲۰۱۶/۱۲/۲۰؛ پذیرش ۲۰۱۷/۷/۹

چکیده:

بزرگ‌نمایی تصویر یکی از مسائل موجود در زمینه پردازش تصویر است که حفظ کیفیت و ساختار تصویر بزرگ‌نمایی شده در آن مهم می‌باشد. در بزرگ‌نمایی تصویر لازم است که پیکسل‌های اضافی در اطلاعات تصویر قرار داده شود. اضافه کردن اطلاعات به تصویر باید با بافت موجود در تصویر سازگار باشد و بلوک‌های مصنوعی ایجاد نکند. در این پژوهش، پیکسل‌های مورد نیاز با استفاده از توابع پایه‌ای شعاعی و محاسبه پارامتر شکل C توسط الگوریتم ژنتیک تخمین زده می‌شوند و سپس تمام پیکسل‌های تخمین زده شده، بر اساس زیر الگوریتم اصلاح لبه مورد بازنگری قرار می‌گیرند. روش پیشنهادی که یک روش غیرخطی محسوب می‌شود، لبه‌ها را حفظ می‌کند و ماتی و مصنوعات بلوکی تصویر بزرگ‌نمایی شده را به حداقل می‌رساند. روش پیشنهادی بر روی چند تصویر برای محاسبه پارامتر شکل مناسب توابع پایه شعاعی مورد ارزیابی قرار گرفته است. نتایج عددی بر روی چند تصویر مختلف با روش‌های دیگر توسط معیار PSNR و SSIM مورد مقایسه و ارزیابی قرار گرفته است. میانگین PSNR مربوط به تصویر اصلی و بزرگ‌نمایی شده $33/16$ می‌باشد که نشان می‌دهد تصویر بزرگ‌نمایی شده با ضریب 2 به تصویر اصلی شباهت زیادی دارد و تاکید می‌کند روش پیشنهادی از کارائی مطلوبی برخوردار است.

کلمات کلیدی: بزرگ‌نمایی تصویر، توابع پایه‌ای شعاعی، الگوریتم ژنتیک، درون‌یابی.